Eur. Phys. J. D **16**, 265–269 (2001)

THE EUROPEAN PHYSICAL JOURNAL D

EDP Sciences

Control of island morphology by dynamic coalescence of soft-landed clusters

C. Bréchignac[1,a], Ph. Cahuzac[1], F. Carlier[1,3], C. Colliex[1,2], M. de Frutos[1], N. Kébaïli[1], J. Le Roux[1], A. Masson[1,3], and B. Yoon[1,2,b]

[1] Laboratoire Aimé Cotton[c], bâtiment 505, Université Paris-Sud, 91405 Orsay Cedex, France
[2] Laboratoire de Physique des Solides[d], bâtiment 510, Université Paris-Sud, 91405 Orsay Cedex, France
[3] Laboratoire de Physico-Chimie des Surfaces[e], 11 rue Pierre et Marie Curie, 75231 Paris Cedex 05, France

Received 1st December 2000

Abstract. The deposition of preformed clusters on surfaces has been established as a new way for growing nano-suctures on surfaces. It has been shown that supported island morphology relies on the dynamics of clusters, during the growth, giving rise to shapes from compact to ramified types. This paper identifies and discusses, in the case of antimony cluster deposits, several processes responsible for the non-equilibrium island shapes: limited kinetic cluster aggregation, size dependent coalescence, "wetting-like behavior" of antimony clusters on antimony islands. Using successive predetermined cluster sizes during the deposition process to synthesize polymorphic structure involves the interplay of those mechanisms.

PACS. 36.40.Sx Diffusion and dynamics of clusters – 68.35.Fx Diffusion; interface formation – 61.46.+w Nanoscale materials: clusters, nanoparticles, nanotubes, and nanocrystals

1 Introduction

Traditional thin-film growth techniques based on atomic or molecular beam deposition have been widely used during several decades for either layer-by-layer growth or island formation [1]. With improvements in surface imaging such as transmission electron microscopy (TEM) and scanning tunneling microscopy (STM), deeper insights are obtained in thin-film growth mechanism, their morphology and their structure.

Very recently, the deposition of preformed clusters has evolved as a new way for growing and structuring materials on surfaces [2,3]. Since incident clusters are preformed objects, their size can be used as a new parameter to monitor non equilibrium morphology for the supported islands which cannot otherwise be obtained at room temperature. It is clear that the mobility of soft-landed clusters on surfaces, even for cluster sizes larger than a few thousands atoms, is one of the key points to secure island formation. Moreover island morphology relies on the dynamics. It is governed by the competition between the total coalescence and the diffusion times of the mobile clusters onto the surface, pointing to the importance of kinetics and defects on island growth and on their morphology. In the light of the example that constitutes antimony clusters soft-landed on graphite, this paper will discuss how to control at nanoscale, structure and morphology of islands from cluster beam deposition.

2 Experiment

Neutral antimony clusters Sb_n are produced by gas-aggregation cluster source and are deposited at low kinetic energy (0.05 eV per atom) on (0001) cleavage surfaces of graphite (HOPG) maintained at room temperature [4].

The cluster size distribution is controlled by oven temperature, pressure and composition of the carrier gas, and nozzle diameter. A pulsed low intensity laser ionizes the cluster distribution which enters a time of flight mass spectrometer for monitoring the size distribution. The cluster size distribution has a dispersion Δn with respect to the average size n close to $\Delta n/n \simeq 0.5$. A crystal quartz microbalance measures the flux of incident neutral clusters. Incident cluster flux is of the order of 10^{10} clusters $\mathrm{cm}^{-2}\,\mathrm{s}^{-1}$ and little varies with cluster size. During the deposition, the vacuum in the chamber is better than 10^{-8} torr. The low kinetic energy of incident clusters as compared to their binding energy per atom ($\simeq 1.35$ eV) prevents from a post deposition fragmentation, and clusters are free to move randomly on the surface for making islands.

[a] e-mail: catherine.brechignac@lac.u-psud.fr
[b] *Present address*: School of Physics, Georgia Tech, 837 State St., Atlanta, GA 30332, USA.
[c] CNRS UPR 3321
[d] CNRS UMR 8502
[e] CNRS ESA 7045

The substrates were cleaned by heating at 500 °C for several hours before cluster deposition. In order to control the number and the size of the islands, we performed nucleation on defects [5]. Surface defects are introduced on graphite by ion irradiation. The density of defects is monitored by the irradiation time. Each defect acts as nucleus for island formation. Increasing the defect density reduces the mean capture zone per defect. As a result, for a given coverage, the number of clusters captured by defect decreases.

Samples prepared at different defect densities and various incident cluster sizes were transferred either in high vacuum for STM images or in the air and observed in a scanning transmission electron microscope (STEM) operating at 100 kV and equipped with a field emission gun. We have prepared thin cleavage surfaces of graphite supported by copper grids for transmission electron microscopy observations. High-angle annular dark-field images have been recorded systematically. There is a linear relationship between local thickness of the material and image signals giving information on the height of the islands.

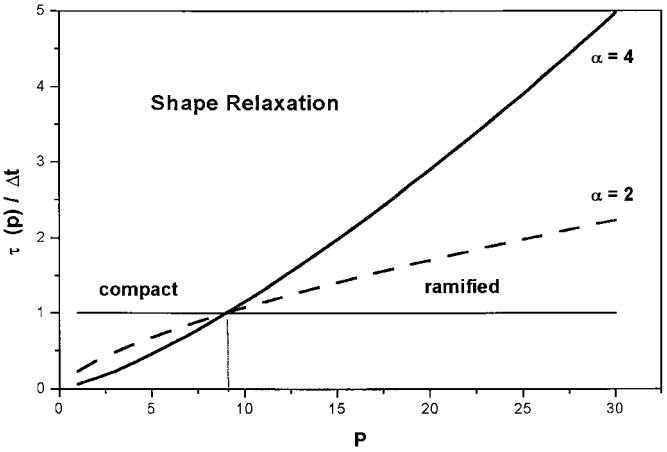

Fig. 1. Variation of the ratio between coalescence Δt and diffusion τ times *versus* the number p of clusters involved in island formation. The cross-over which occurs for $\tau/\Delta t = 1$ separates the island morphologies into two different regimes: the compact island shapes for $\tau/\Delta t < 1$ and the ramified shapes for $\tau/\Delta t > 1$.

3 Results and discussion

3.1 Island morphology induced by kinetic limitation

In the case of nucleation and growth on surface defects, each defect is a nucleation site for island growth by cluster aggregation. In the course of the growth, an island transforms continuously its shape by incorporating new clusters. The process of island formation is governed by two characteristic times: an arrival time Δt defined as the interval time between successive arrivals of clusters to an island, and a coalescence time $\tau(R, n)$ for a n-atom cluster of radius $r = r_0 n^{1/3}$ to entirely coalesce with a spherical island of radius R, resulting in a larger spherical island. As time is going the number p of clusters forming an np-atom island increases linearly with time, its size increases as $R = r_0(np)^{1/3}$. For given deposition conditions (cluster size, flux, temperature, surface defect density, ...) the arrival time is almost constant with R, at least for a certain range of R, whereas the coalescence time increases with R. Macroscopic theories of sintering *via* surface diffusion predict that the coalescence time varies as R^4 for two identical spheres [6]. More generally, for two spheres with different radius, we can write $\tau(R, r)$ proportional to R^α [7]. When Δt is longer than τ, the island reaches a compact spheroid shape before another cluster arrives. In the opposite case, the island does not have time to reach a compact shape before the arrival of the next cluster and evolves towards a non-compact or ramified shape. From the relative variation of $\tau/\Delta t$ as a function of R, there exists a critical island radius R_c and consequently a critical number p_c of clusters for which the cross-over occurs when $\tau = \Delta t$. Compact islands are obtained for p smaller than p_c, dendritic above. Fig. 1 shows the competition between compact and ramified shape relaxation resulting from preformed cluster deposited on surface.

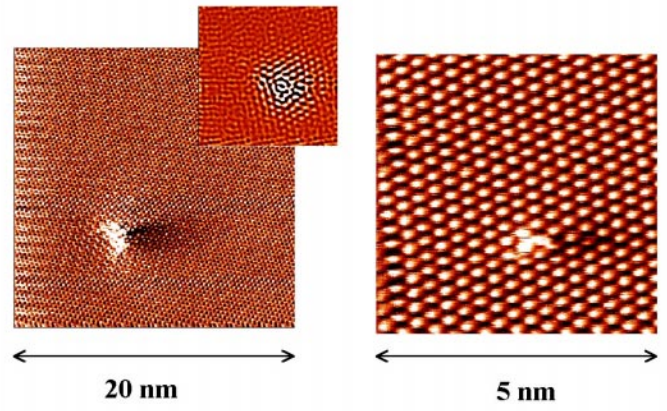

Fig. 2. STM atomic resolution images of defects on graphite where clusters are trapped. Two kinds of defects have been observed: the point defect (right image) and the extended ones (left image). The inset of the left image presents the filtering in the Fourier space enhancing the surface reconstruction.

In order to verify this kinetic model we have performed nucleation on defects. Fig. 2 shows STM images of defects on graphite (HOPG) with atomic resolution. Two kinds of defects are observed. 90% are extended over a few nanometers with a $\sqrt{3} \times \sqrt{3}$ reconstructed graphite surface, less than 10% are point defects involving only few carbon atoms. For given flux and coverage (1.5 ML) a neutral cluster distribution of antimony Sb_n peaking at $n = 500$ is deposited on several irradiated surfaces with different defect densities.

Varying the defect density N_d, *i.e.* the mean capture area per defect, we limit the number of clusters making islands and vary the delay time between two successive arrivals in the capture zone, $\Delta t_0 = N_d/\Phi$, where Φ is the cluster flux. Since the cluster flux little varies in our

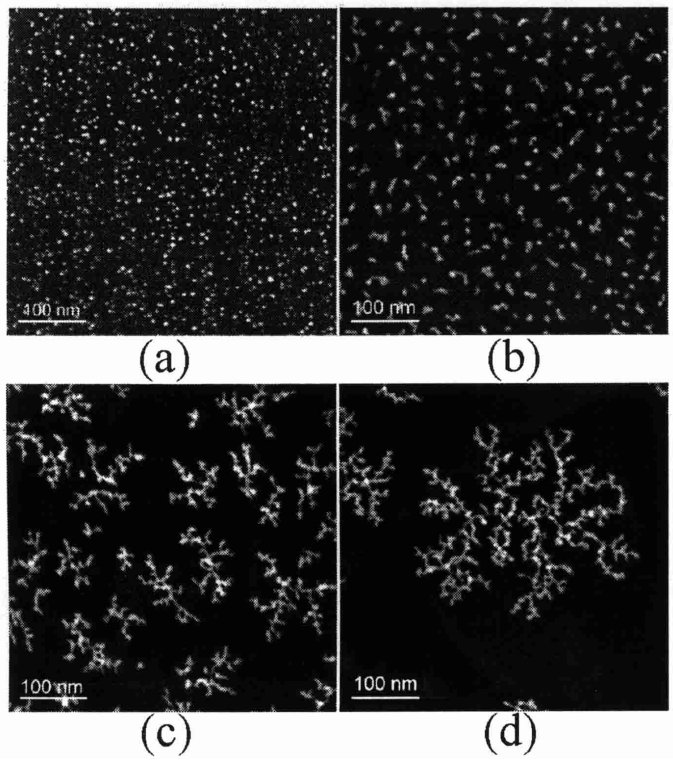

Fig. 3. STEM Images of four films of deposited 500-atom clusters (1.5 ML) on different irradiated graphite. As the number of defects decreases (decreasing the irradiation time) the shape of the islands transforms from compact to ramified.

experimental conditions, only a substantial variation of the defect density gives rise to a noticeable change of the kinetic effects on the island growth. However, the full understanding of the kinetic of island growth requires to take into account the cluster diffusion in the capture zone for reaching the island. From the diffusion coefficient D previously obtained for antimony clusters moving on graphite ($D = 1.18 \times 10^{-6}$ cm^2 s) [8], we can estimate the time for exploring a capture zone $t_d = (1/D)N_d$. In most cases in our experiment, this value is smaller than Δt_0.

At a large defect density ($N_d = 3.5 \times 10^{11}$ cm^{-2}), leading to small capture area per defect, only few clusters reach each capture zone, and have time to aggregate into small islands having compact shapes with diameter less than 5 nm (Fig. 3a). Decreasing the number of defects ($N_d = 10^{11}$ cm^{-2}), consequently increasing the capture zone, a larger number of clusters are involved in island formation which begin to arm-like growth extending from a core of $2R_c = 6$ nm (Fig. 3 b). At small defect density ($N_d < 10^{10}$ cm^{-2}) large islands grow with fractal shape while maintaining a constant arm-width of 6 nm. Fig. 3 presents several stages of the transformation from compact to fractal shapes as the number of involved clusters increases in agreement with the kinetic model. It is interesting to note that our results behave in a similar way as those previously obtained for two dimensional growth of Au on Ru(0001) in a sub-monolayer range. In that case the restricted diffusion of Au atom implies fractal growth when the edge diffusion Au/Au island is sufficiently low while surface diffusion of Au/Ru(0001) is still appreciable [9].

3.2 Island morphology induced by cluster size

In order to explain in size selected cluster deposition, the constant arm-width R_c of the dendrites we assume that the coalescence is governed by the diffusion of the atoms constituting the cluster on the surface of the existing island. The surface of the island which can be explored by the atoms of the incident cluster during the delay time between two successive arrivals gives rise to a "restricted wetting-like" behavior. For small-numbered atom clusters, most of the atoms spread over the surface island leading to a complete wetting. For large-numbered atom clusters, most of the atoms remain together leading to a local shape modification. The shape modification of non-compact islands behaves locally in the same way as compact ones by replacing island radius R by the inverse of local curvature of shape modification region. Therefore, the growing front continues to evolve until it reaches the value where $\Delta t = \tau(R_c, n)$ leading to a local curvature of $1/R_c$ [4].

The coalescence time between an incident cluster and growing island depends on both island and incident cluster size. It increases as cluster size increases. Assuming that the arrival time $\Delta t(n)$ of a n-atom cluster on graphite, for a given defect density, varies less rapidly than the coalescence time, the critical island radius $R_c(n)$ for the cross-over transition between compact and ramified shape increases as n decreases. Fig. 4 shows electron microscopy images for different antimony cluster size depositions. Since we have shown that the arm thickness of the dendrites equates the critical diameter $2R_c$, we deduce the critical number p_c of clusters required for such a transition at different cluster sizes.

Fig. 5 presents the power law behavior of p_c *versus* n in a logarithmic plot. It shows evidence of a strong variation of the coalescence time with cluster size. The extrapolation of the straight line to $p_c = 1$ *i.e.* $\ln(p_c) = 0$, gives the cluster size n_c beyond which the island grows in a pure diffusion-limited aggregation regime (DLA) [10]. In this case the clusters perform random walks until they encounter an island and stick with no further coalescence. It has to be noted that this value $n_c = 1300$ is in agreement with previous results from ref. [8].

3.3 Polymorphic islands

The control of island morphology by changing the incident cluster size can be used to synthesize polymorphic objects by sequential depositions of clusters of two different average sizes.

For Fig. 6a we have only deposited antimony clusters Sb_n of $n = 90$ whereas Fig. 6b shows the result of two successive depositions, first $n = 90$ then $n = 500$. Dimorphic islands containing distinct structures have been obtained. Each island is made of a thick central part with

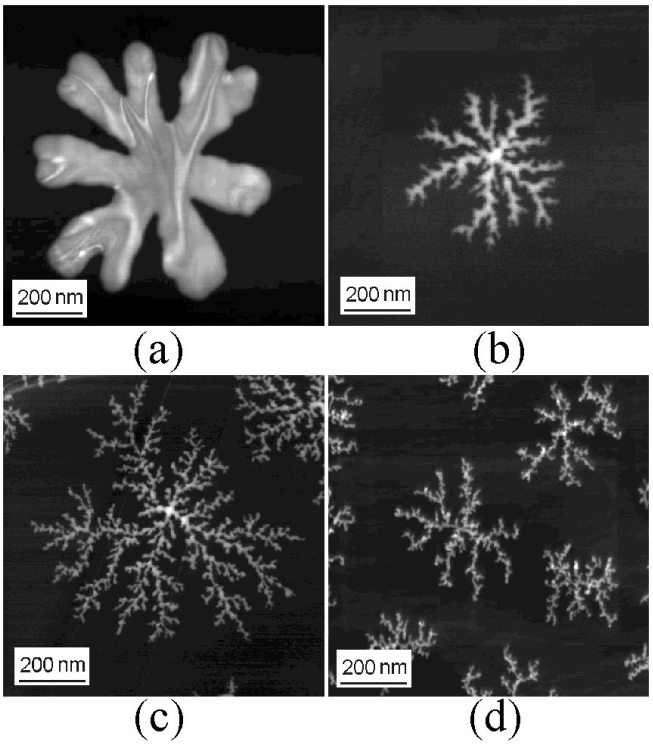

Fig. 4. STEM images of island morphologies obtained for different incident cluster sizes. (a) $n = 90$, (b) $n = 150$, (c) $n = 500$ and (d) $n = 1400$.

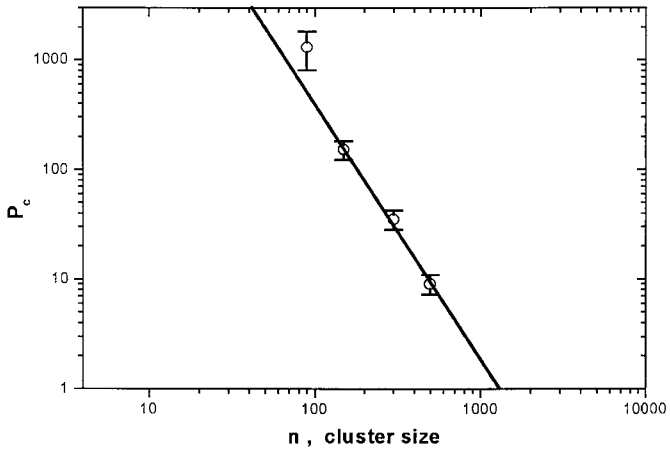

Fig. 5. Critical number p_c of clusters for the cross-over island shape transition *versus* incident cluster size n, in a log-log plot. The intercept of the straight line with the n axis gives the cluster size beyond which the pure diffusion-limited aggregation without coalescence prevails.

a seaweed-like shape and of thinner outer branches, with 30 nm and 6 nm arm-width respectively. These values coincide with those obtained for single cluster size depositions showing only a juxtaposition of the two morphologies. The fact that the incident 500-atom clusters little affect the preexisting seaweed-like core is due to a "limited wetting" of the cluster on the core. As a 500-atom cluster reaches the island the atoms constituting the cluster explore or partially wet the core, causing instability. The resulting shape modification is an increase of the local radius. As the cluster deposition is going the local radius increases until it reaches the critical value $R_c(500)$ imposed by $\Delta t(500)/\tau(500) = 1$ when dendritic growth occurs. Since $R_c(500)$ is significantly larger than $R_c(90)$ only small perturbations affect the central core leading to a juxtaposition of the two morphologies.

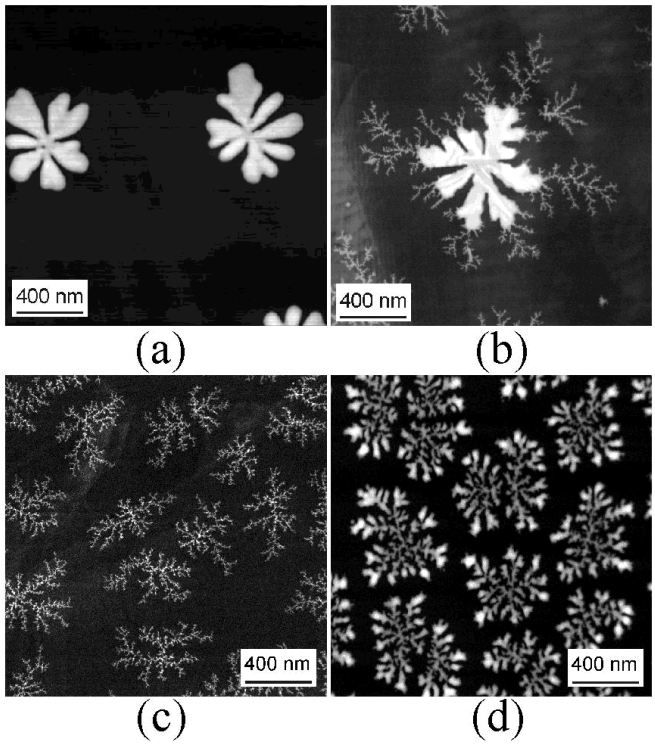

Fig. 6. STEM images of four films after sequential depositions of different cluster sizes Sb_n. (a) $n = 90$, (b) $n = 90$ followed by $n = 500$, (c) $n = 500$, (d) $n = 500$ followed by $n = 90$. It is clearly seen that in (b) the addition of Sb_{500} forms dendrites on the island core without affecting the island core, whereas in (d) the consequent addition of Sb_{90} strongly perturbs the fractal core.

Such a result contrasts with that obtained when the reversed deposition procedure was applied. In Fig. 6c we have only deposited antimony clusters Sb_n with $n = 500$ whereas in Fig. 6d two successive depositions have been performed first $n = 500$ then $n = 90$. We have not only observed the juxtaposition of the two morphologies *i.e.* thin dendritic core with seaweed-like endings. In large-then-small cluster deposition, a noticeable amount of thickening has occurred in the fractal core. Since $R_c(90)$ is smaller than $R_c(500)$ the arrival of 90-atom-cluster on a fractal skeleton with arm-width thinner than $R_c(90)$ strongly affects the skeleton. The 90-atoms entirely wet the fractal arm and thicken the arm. Moreover the fractal island cores spread over a large graphite surface, hence a significant part of successive deposited 90-atom-clusters can impinge onto existing fractal islands. They diffuse between the fractal arms and capillary merge along the arms. Those

which arrive between fractal islands contribute to grow the endings. We have recently shown that such a complex pattern which is formed from successive intrinsically non equilibrium phenomenon is particularly unstable leading to restructured crystallized islands.

4 Conclusion

Our size control of deposited antimony clusters on graphite supports a "dynamical coalescence growth picture" which is an intrinsically non equilibrium phenomenon. This allows the formation of complex patterns. Restricting the surface of the cluster diffusion on graphite by injecting surface defects, points out the transition between compact and ramified shapes as island grows. Changing the kinetic of the growth by varying cluster size during the deposition process, creates polymorphic islands which are governed by the wetting like behavior of the incident clusters on the preformed islands.

References

1. J.A. Venables, G.D.T. Spiller, M. Hanbücken, Rep. Prog. Phys. **47**, 399 (1984).
2. See, for example, *Proceedings of ISSPIC9*, edited by J.M. Bonard, A. Châtelain, Eur. Phys. J. D **9**, 1 (1999).
3. P. Jensen, A.L. Barabasi, H. Larralde, S. Havlin, H.E. Stanley, Phys. Rev. B. **50**, 15316 (1994).
4. B. Yoon, V.M. Akulin, Ph. Cahuzac, F. Carlier, M. de Frutos, A. Masson, C. Mory, C. Colliex, C. Bréchignac, Surf. Sci. **443**, 76 (1999).
5. P.A. Mulheran, J.A. Blackman, Phil. Mag. Lett. **74**, 4694 (1995).
6. F.A. Nichols, J. Appl. Phys. **37**, 2805 (1966).
7. G. Rosenfeld, K. Morgenstern, M. Esser, G. Comsa, Appl. Phys. A **69**, 489 (1999).
8. L. Bardotti, P. Jensen, A. Hoareau, M. Treilleux, B. Cabaud, Phys. Rev. Lett. **74**, 4694 (1995).
9. R.Q. Hwang, J. Schröder, C. Günther, R.J. Behm, Phys. Rev. Lett. **67**, 3279 (1991).
10. T.A. Witten, L.M. Sanders, Phys. Rev. Lett. **47**, 1400 (1981); Phys. Rev. B **27**, 5686 (1983).